

AD-A102 628

MASSACHUSETTS INST OF TECH CAMBRIDGE DEPT OF MATERIA--ETC F/6 11/6  
MOLECULAR ORBITALS AND THE ATOMISTICS OF FRACTURE.(U)

JUL 81 M E EBERHART, K H JOHNSON, R P MESSMER N00014-81-K-0499

NL

UNCLASSIFIED TR-1

1 or 1  
40.9  
026.28

END  
40.9  
026.28  
9-81  
DTIC

AD A102628

DTIC FILE COPY

REPORT DOCUMENTATION PAGE			READ INSTRUCTIONS BEFORE COMPLETING FORM
1. REPORT NUMBER 1	2. GOVT ACCESSION NO. AD-A102628	3. RECIPIENT'S CATALOG NUMBER	
4. TITLE (and Subtitle) Molecular Orbitals and the Atomistics of Fracture.	5. TYPE OF REPORT & PERIOD COVERED Interim		
6. AUTHOR(s) M. E. Eberhart, K. H. Johnson, R. P. Messmer and C. L. Briant	7. CONTRACT OR GRANT NUMBER(S) N00014-81-K-0499		
8. PERFORMING ORGANIZATION NAME AND ADDRESS Department of Materials Science and Engineering, N.I.T., and General Electric Co., Corporate Research and Development, Schenectady, NY 12301	10. PROGRAM ELEMENT, PROJECT, TASK AREA & WORK UNIT NUMBERS Task No. NR 056-757		
11. CONTROLLING OFFICE NAME AND ADDRESS Office of Naval Research Department of the Navy Arlington, Virginia 22217	12. REPORT DATE July 26, 1981		
14. MONITORING AGENCY NAME & ADDRESS (if different from Controlling Office) <b>LEVEL</b>	15. SECURITY CLASS. (of this report)		
	15a. DECLASSIFICATION/DOWNGRADING SCHEDULE		
16. DISTRIBUTION STATEMENT (of this Report) Approval for public release; distribution unlimited.			
17. DISTRIBUTION STATEMENT (of the abstract entered in Block 20, if different from Report)	DTIC ELECTE S AUG 1 0 1981		
18. SUPPLEMENTARY NOTES	C		
19. KEY WORDS (Continue on reverse side if necessary and identify by block number) grain boundary; embrittlement; SCF-X <sub>a</sub> -SW method.			
20. ABSTRACT (Continue on reverse side if necessary and identify by block number) Self-consistent-field Xalpha scattered-wave (SCF-X <sub>a</sub> -SW) cluster molecular-orbital models have been constructed for grain-boundary embrittlement of metals. Two specific examples are presented: (1) the embrittlement of nickel by sulfur and (2) the embrittlement of iron by hydrogen.			

OFFICE OF NAVAL RESEARCH  
Contract N00014-81-K-0499  
Task No. NR 056-757

TECHNICAL REPORT NO. 1 ✓

Molecular Orbitals and the Atomistics of Fracture

by

M. E. Eberhart and K. H. Johnson  
Department of Materials Science and Engineering  
Massachusetts Institute of Technology  
Cambridge, Massachusetts 02139  
and  
R. P. Messmer and C. L. Briant  
General Electric Company  
Corporate Research and Development  
Schenectady, New York 12301

July 28, 1981

Reproduction in whole or in part is permitted for  
any purpose of the United States Government

Approved for Public Release: Distribution Unlimited

Accession For	<input checked="" type="checkbox"/>
NTIS GR&I	<input type="checkbox"/>
DTIC TAB	<input type="checkbox"/>
Unannounced	<input type="checkbox"/>
Justification	<input type="checkbox"/>
By	
Distribution/	
Availability Codes	
Avail after	
Dist Specified	

A

## MOLECULAR ORBITALS AND THE ATOMISTICS OF FRACTURE

M. E. Eberhart and K. H. Johnson

Department of Materials Science and Engineering  
 Massachusetts Institute of Technology  
 Cambridge, MA 02139

R. P. Messmer and C. L. Briant

General Electric Company  
 Corporate Research and Development  
 Schenectady, NY 12301

### INTRODUCTION

If a metal contains very few impurities and is mechanically tested in an inert environment, its fracture mode will be either transgranular cleavage or transgranular ductile microvoid coalescence. If, however, the metal is of commercial purity, the brittle fracture mode can switch from cleavage to intergranular separation. This transition is undesirable because intergranular fracture is generally a very low energy process.

The occurrence of intergranular fracture in a specific situation will depend on a number of metallurgical variables: grain size, yield strength, test temperature, and notch radius. However, in all reported cases, one observation is common. Impurities which have a very low solubility in the bulk have segregated to the grain boundaries and weakened them. The bulk concentration of these impurities need only be several hundred ppm for grain boundary concentrations of 5-10 atomic percent to be observed. Examples of this impurity-induced weakening of grain boundaries include sulfur in iron and nickel, phosphorus, tin, and antimony in steel, bismuth in copper, and oxygen in refractory metals.

If the environment is not inert, intergranular separation may occur even though the fracture mode in an inert environment would

be transgranular. One much studied example of this is hydrogen embrittlement. If a sample is tested either in hydrogen gas, or is cathodically charged with hydrogen and then tested in an inert environment, one finds that the mechanical properties of the material are often degraded and that the fracture mode has become more intergranular. As with impurity-induced embrittlement, many additional variables can affect the degree to which hydrogen will cause embrittlement, and one of the worst possible cases is to have both hydrogen and impurities segregated at the grain boundaries. However, it is clear that hydrogen must segregate at interfaces and reduce the cohesive strength across them.

We believe that an important contribution to understanding some aspects of these complex problems of embrittlement in metals can be made through theoretical studies of bonding in model systems. The philosophy is to isolate groups of atoms in clusters which simulate a possible local environment of interest and to perform detailed quantum mechanical calculations using molecular orbital theory to probe the nature of the chemical bonding.

After discussing molecular orbital theory and the X<sub>a</sub>-scattered-wave technique in the next section, we consider in the following sections two recent applications of this approach to models of potential metallurgical interest.

#### MOLECULAR ORBITAL THEORY AND THE SCF-X<sub>a</sub>-SW CLUSTER METHOD

The most characteristic feature of molecular orbital theory is that it provides an independent-particle interpretation of the electronic structure of a molecule or solid. That is, each electron of the system has associated with it a characteristic spin-orbital and energy level which are determined by solving Schrödinger's equation for an electron in the average potential energy of all the other electrons in the system. The most familiar of such techniques is the Hartree-Fock self-consistent field method, in which each molecular orbital is traditionally represented by a linear combination of atomic orbitals (the HF-SCF-LCAO method). For all but the simplest molecules one must, at least for the present, choose atomic-orbital basis sets which are fairly far from the correct solutions of the Hartree-Fock Schrödinger equations. We refer to this type of approximate solution of the Hartree-Fock equations using the LCAO representation as the AHF-SCF-LCAO method.

It is well known that the Hartree-Fock theory provides a poor description of the electronic structure of a molecule or solid at large internuclear distances and that it leads to an improper description of the dissociation of such systems. In order to correct for this behavior, it is necessary for one to work with linear combinations of Slater determinants of molecular orbitals, the

so-called "configuration-interaction" (CI) procedure, which is not only complicated computationally, but also destroys the independent-electron interpretation. A further difficulty is that in performing numerical calculations using the LCAO approximation at either the AHF or CI levels of sophistication, the number of two-electron multicenter integrals which must be calculated even for moderately sized systems becomes enormous. For example, in a recent calculation on a molecule consisting of 26 atoms, all of atomic numbers less than ten,  $10^{11}$  integrals had to be evaluated and the calculations required the equivalent of 192 h on an IBM 360/195 computer, one of the fastest machines available.

A much more practical independent-electron theory, which avoids most of the difficulties associated with the AHF-SCF-LCAO and CI methods, is the recently developed SCF-X<sub>a</sub>-SW cluster method. Based on the combined use of Slater's X<sub>a</sub> statistical theory of exchange correlation and Johnson's multiple-scattered-wave formalism, this technique allows one to calculate accurate self-consistent spin-orbital energies, wave functions, charge densities, and total energies for complex molecules and clusters, yet requires only relatively small amounts of computer time. Like the AHF-SCF-LCAO approach, the SCF-X<sub>a</sub>-SW method is an approximate theory of many-electron systems, but it is not an approximation to Hartree-Fock theory. First of all, in contrast to HF theory, the X<sub>a</sub> statistical expression for the total many-electron energy automatically goes to the proper separated-atom limit as the internuclear distances are increased to infinity, i.e., as the system dissociates. Second, it has been shown that the X<sub>a</sub> theory satisfies Fermi statistics, thereby ensuring the proper ordering and occupation of electronic energy levels, while the HF theory does not. Third, it has been proven that, under the proper conditions, the X<sub>a</sub> statistical total energy rigorously satisfies both the virial and Hellmann-Feynman theorems, which facilitates the calculation of the equilibrium cohesive energies of molecules and solids. Finally, the SCF-X<sub>a</sub>-SW method, in conjunction with the "transition-state" concept, leads to an accurate approximate description of the excited electronic states and charge distributions of polyatomic systems, including the effects of orbital relaxation which are usually neglected in applying Koopmans theorem in the AHF-SCF-LCAO approach.

The SCF-X<sub>a</sub>-SW method and transition-state procedure have already been applied successfully to a wide range of molecules and clusters in solids. Because the required computational effort does not increase inordinately with the number of electrons per atom or with the number of atoms in the molecule or cluster, the SCF-X<sub>a</sub>-SW method is ideally suited for describing the electronic structures of transition-metal complexes and clusters representing the local molecular environment of a grain boundary.

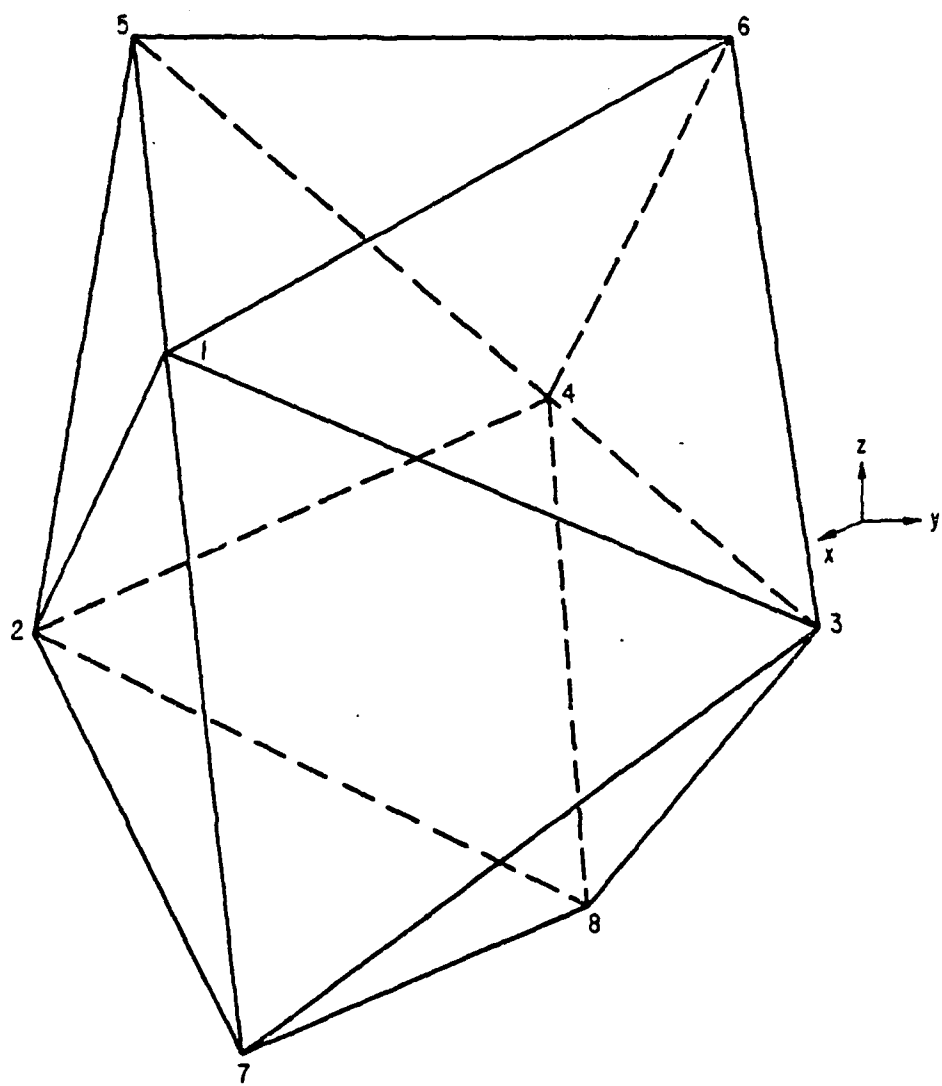


Figure 1

MOLECULAR ORBITAL MODEL FOR GRAIN BOUNDARY EMBRITTLEMENT OF NICKEL  
BY SULFUR

As discussed in the last section, the theoretical method we use to investigate the electronic structure of the local environment at a grain boundary consists of two parts. The first is to use a cluster of atoms to represent the local environment and the second is to use molecular orbital theory to solve for the electronic structure of the cluster of atoms.

To apply this technique to grain boundaries one must first choose a cluster that resembles in some way the local environment an impurity atom might have were it at the grain boundary. The choice of such clusters is considerably simplified due to the recent work of Ashby, Spaepen, and Williams, who have shown that the structure of grain boundaries in fcc solids can be described in terms of atoms at the vertices of Bernal deltahedra. The individual deltahedra are small clusters containing four to thirteen atoms and thus provide a natural initial model of local atomic structure with which to investigate the electronic properties by SCF-X<sub>α</sub>-SW calculations. In order to investigate the feasibility of applying such methods to this problem we have chosen to use one particular cluster in this work.

The particular cluster we chose is the tetragonal dodecahedron shown in Fig. 1. It contains eight atoms and has D<sub>2d</sub> point group symmetry. We do not claim that this structure is necessarily a prevalent one in grain boundaries. However, it does contain four atoms (numbered 1, 2, 3, and 4) slightly but symmetrically displaced from the x-y plane and four other atoms further displaced from this plane. One can roughly consider that the four atoms nearest the x-y plane are grain boundary atoms and that the other four are in the first atomic layers away from the precise boundary.

It is well established experimentally that sulfur embrittles nickel. In order to investigate the electronic effects of a sulfur atom at a grain boundary in Ni, we have carried out two calculations on a model system in which the Ni atoms were placed at each of the eight sites of the cluster shown in Fig. 1 with an internuclear separation of 2.49 Å. In the first calculation, we considered the cluster containing only the eight nickel atoms. For the second calculation, a sulfur atom was placed at the center of the cluster. An interstitial site of this type is a possible position which a sulfur atom would choose at a grain boundary. For these two configurations we have determined the molecular orbitals for the clusters, their corresponding energy levels, and the valence charge densities.

The energy levels for each cluster are shown in Fig. 2. We note that in the Ni<sub>8</sub>S cluster several of the energy levels have

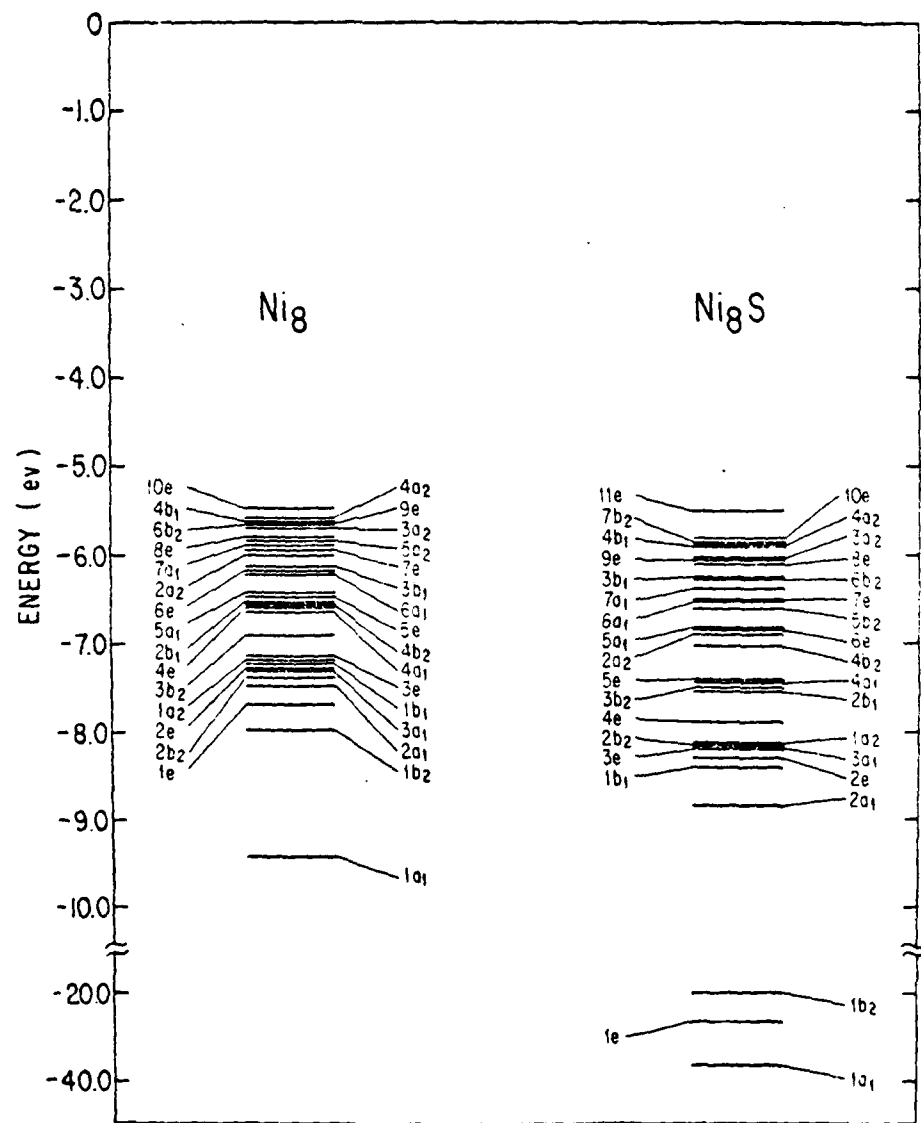


Figure 2

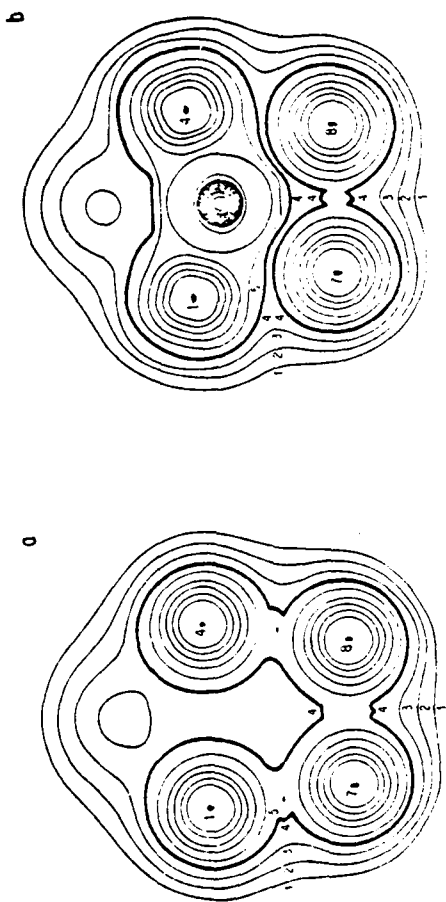
been lowered substantially. Those that have been lowered have orbital wave functions which are highly localized on the sulfur atom and its four nearest neighbors, i.e., the four nickel atoms closest to the x-y plane. Based on this simple analysis one might assume that some Ni-Ni bonds have been weakened.

The bonding may be better understood if one analyzes the molecular orbitals of the clusters in more detail; however, in this particular case a more succinct picture of the bonding in the cluster can be obtained by summing the orbital charge densities over all the occupied valence orbitals. One can then plot contours of the total valence charge density which exists on any plane. These are shown in Fig. 3 for the x-z plane. In this figure we have plotted the same set of contours for both clusters. The three outermost contours (numbered 1, 2, and 3) in both clusters surround all atoms. However, contour number 4 (which is shown with a heavier line for clarity) is quite different in the two clusters. In Ni<sub>8</sub>, it shows bonding between the pairs of nickel atoms 1 and 7, 7 and 8, and 4 and 8, where the characteristic "neck" regions between the pairs of atoms is responsible for bonding. In Ni<sub>8</sub>S, the shape of contour number 4 is quite different. The characteristic neck bonding region between atoms 1 and 7, and 4 and 8 is gone and consequently so is the concomitant strong bonding between the two types of nickel atoms. Furthermore, the size of the neck region between atoms 7 and 8 is reduced from that in Ni<sub>8</sub>, implying a weakening of this metal-metal bond as well. Contour 4 in Ni<sub>8</sub>S is split into two distinct regions. The upper region of contour 4 and an inner contour of the nickel atoms nearest the sulfur atom enclose both the nickel atoms and the sulfur. This would lead to very strong bonds between this set of nickel atoms and the sulfur. However, there is no such bonding interaction between the sulfur atoms and the other nickel atoms.

From these results a clear picture begins to emerge. Adding sulfur to the cluster of nickel atoms causes strong Ni-S bonds to be formed between the nickel atoms nearest the sulfur. Yet this weakens bonds which the nickel atoms would ordinarily have with the other nickel atoms that are not as close to the sulfur atom. In this cluster the strong Ni-S bonds involve the sulfur atom and the four nickel atoms nearest the x-y plane. We suggested earlier that these atoms might be thought of as being in the grain boundary. However, the bonds between the nickel atoms nearest the x-y plane and those farther away are weakened. These bonds might represent those from the boundary out to the first layer of the bulk. Clearly, if those are weakened, the stress required for fracture would be less.

Therefore, based on the calculations we can suggest an electronic mechanism by which grain boundary embrittlement could occur. We stress that these are the results from calculations on only one

Figure 3



system. Furthermore, we have chosen an embrittling element which probably occupies an interstitial site at the grain boundary. Other embrittling elements would clearly be substitutional. Also, many other types of geometrical configuration are possible at the boundary. Yet, with these results, we believe that it is not presumptuous to propose that the above-described mechanism is one mechanism by which segregated elements embrittle the grain boundary.

#### MOLECULAR ORBITAL MODEL FOR HYDROGEN EMBRITTLEMENT OF IRON

The causes and mechanisms of hydrogen embrittlement have been and will continue to be the subjects of detailed investigation. As a result, several models have been offered in explanation of the embrittlement phenomenon. These models, however, cannot account for embrittling at the atomic level, as a chemical interaction between hydrogen and the embrittled metal. It is the purpose of this paper to present the results of SCF-X<sub>a</sub>-SW molecular-orbital calculations on iron-hydrogen clusters in order to explain hydrogen embrittling of ferrous alloys at the most fundamental level.

Hydrogen atoms are most frequently found in octahedral holes of transition metals. If molecular hydrogen were adsorbed within tetrahedral holes then concerted dissociation of molecular hydrogen would result in placing atomic hydrogen in octahedral holes. Accordingly, the four-atom iron cluster shown in Fig. 4 will be used to model the tetrahedral hole and the site for hydrogen adsorption in bcc iron. (Both the tetrahedral and octahedral holes of bcc iron are misnamed since they actually present a D<sub>2d</sub> and tetragonal symmetry respectively.) In an earlier paper, the results of SCF-X<sub>a</sub>-SW molecular-orbital calculations of four-, nine-, and fifteen-atom clusters of iron were presented. It was shown that these clusters provide a model for the local electronic structure of bcc iron. A comparison of these results indicates that both the four-atom and fifteen-atom clusters exhibit the large exchange splitting and high magnetic moment characteristic of bulk iron. Net spin electron number per atom for Fe<sub>15</sub> is 2.7 and for the Fe<sub>4</sub> cluster 2.5 compared with 2.12 for the bulk. The density of states in the four-atom cluster is sufficiently similar to the density of states in the 15-atom cluster to justify the use of Fe<sub>4</sub> as a model for a site of hydrogen adsorption. It is important to note that the fifteen-atom cluster provides three environments for the atoms of the cluster. In bulk iron (neglecting surface effects) each iron atom is in the same environment. It is this fact which is responsible for the variation of properties predicted by the cluster method with those measured in bulk iron. In a calculation of this type, however, where an impurity is being modeled, the impurity breaks the symmetry of the bulk and there are a number of environments around the impurity site. As a result, the cluster method is ideally suited for the study of dilute impurity states and

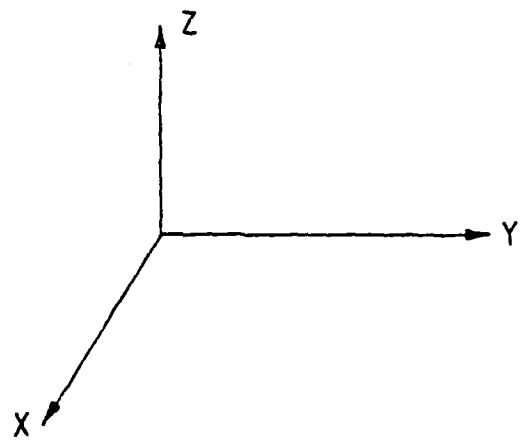
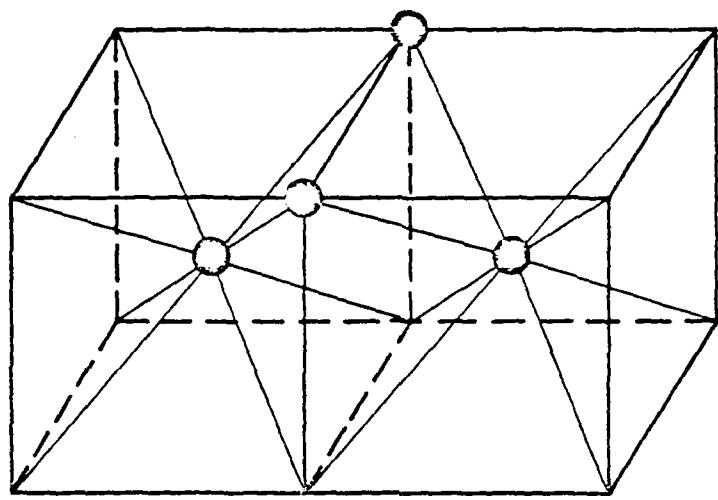


Figure 4

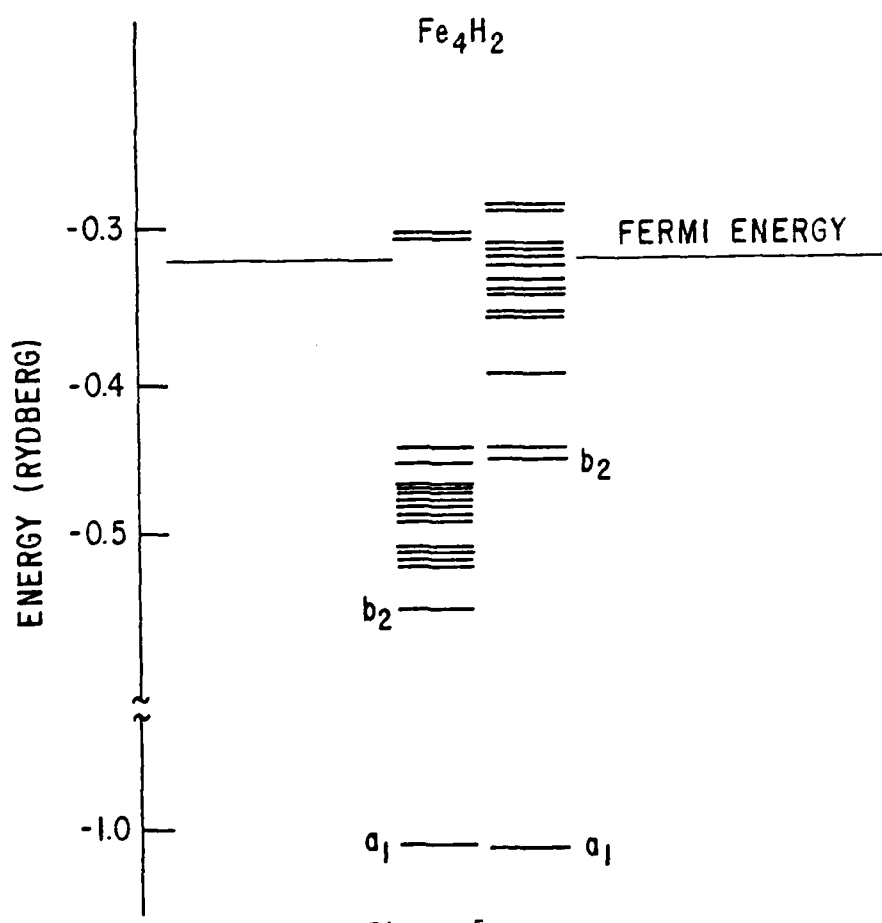
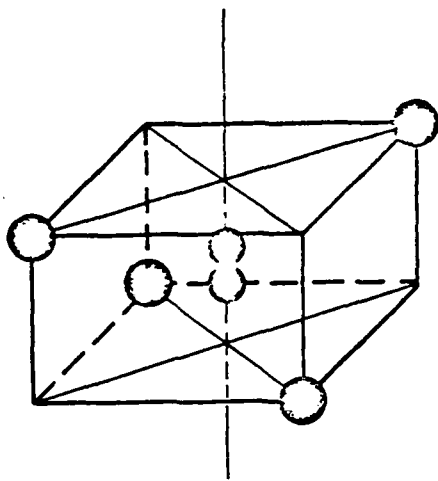


Figure 5

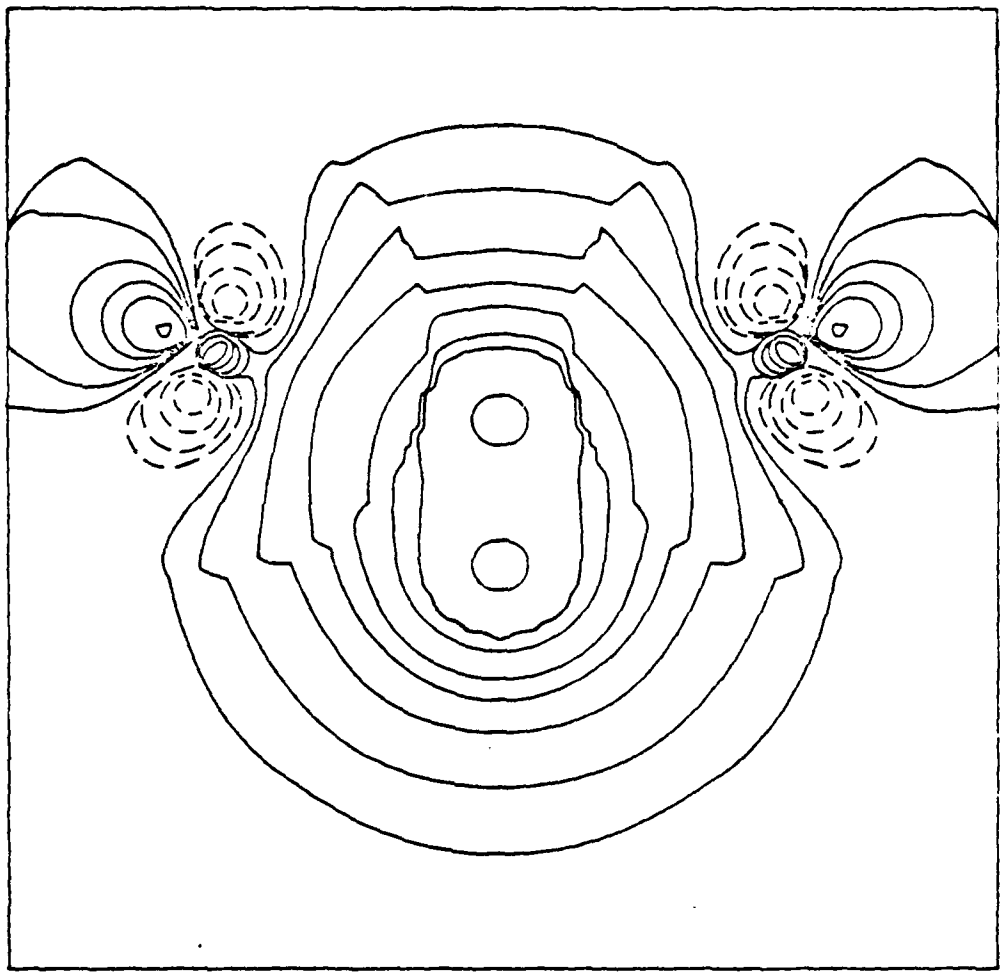


Figure 6

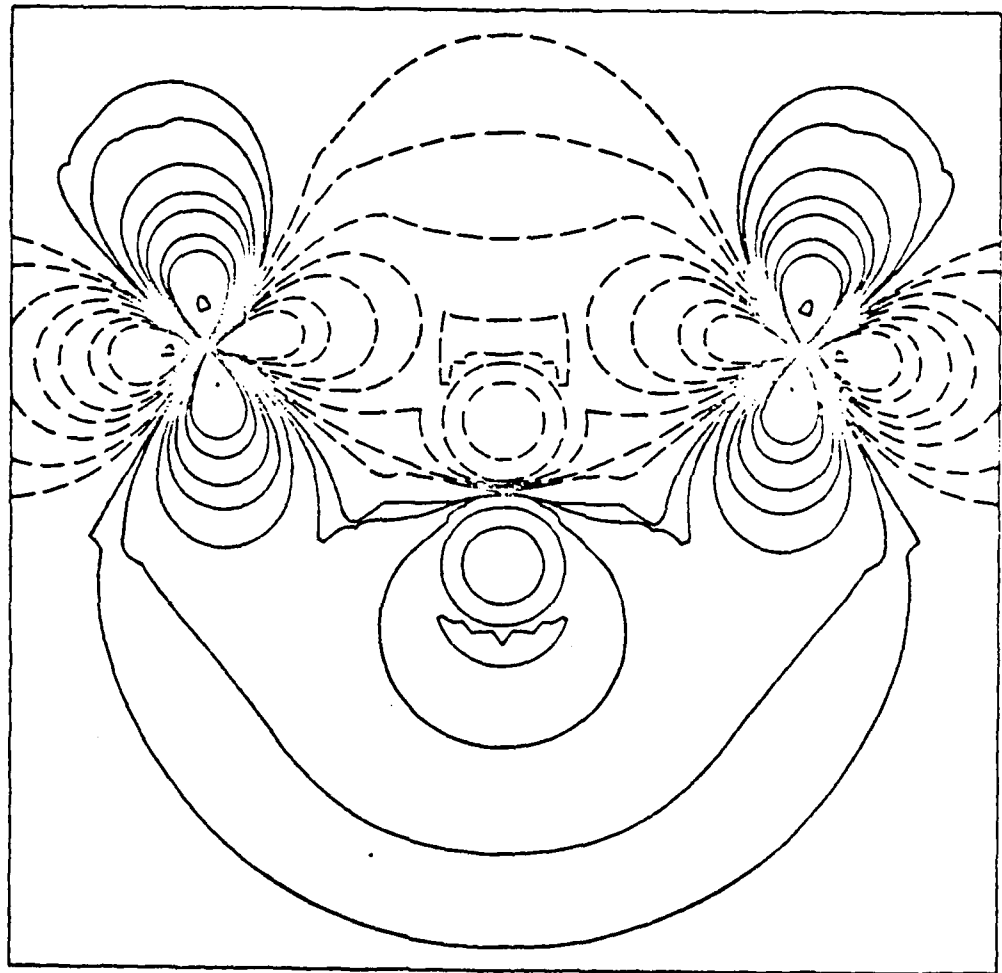


Figure 7

consequently smaller clusters than those used in the study of bulk properties can be used.

The molecular-orbital energy levels of a hydrogen molecule inserted into the four-atom cluster is shown in Fig. 5. The  $a_1$  and  $b_1$  orbitals of the four-atom iron cluster have the same symmetry as the hydrogen molecule bonding and antibonding orbitals. These hydrogen molecular orbitals couple with the lowest lying  $a_1$  and  $b_2$  orbitals of the  $Fe_4$  cluster to produce the molecular orbitals shown in Figs. 6 and 7. As a result of this coupling the lowest lying  $a_1$  and  $b_2$  orbitals of  $Fe_4H_2$  are stabilized relative to the position of these orbitals in  $Fe_4$ . The  $a_1$  orbital is predominantly a H-H bonding orbital the H-Fe interaction is non-bonding. The  $b_2$  orbital in the  $Fe_4$  cluster is d-d  $\pi$ -bonding between nearest neighbors and  $\delta$ -bonding between second-nearest neighbors. The addition of  $H_2$  strengthens the bonding interaction between second-nearest neighbors, has little effect on the nearest-neighbor interaction, and is strongly antibonding between the hydrogen atoms. The H-H distance in this cluster is the molecular H-H distance. This is the distance which is realized when there is no electron density in a H-H antibonding orbital. In this cluster some of the electron density from the metal cluster  $b_2$  orbital is transferred into the antibonding orbital of the hydrogen molecule. The hydrogen molecule H-H distance is no longer a stable equilibrium distance and the hydrogen atoms will begin to dissociate. All transition metals are known to dissociate hydrogen molecules. The efficiency of this dissociation will depend on the amount of overlap between the metal orbital of suitable symmetry and the antibonding orbital of the hydrogen molecule. Other than the low-lying  $a_1$  and  $b_2$  orbitals, no other orbitals of this cluster have any significant hydrogen admixture. Two additional spin orbitals are occupied, however, by the two electrons contributed by the hydrogen molecule.

Figure 8 gives the molecular orbital energy levels for the same arrangement of iron atoms but now the H-H distance has been increased as a consequence of the electron density in the H-H antibonding orbital. Again the lowest lying  $a_1$  orbital is the only orbital with significant H-H bonding contributions (Fig. 9). The lowest lying  $b_2$  orbital is H-H antibonding, as in the previous case, but this interaction has been lessened as is clearly seen in Fig. 10. There is a reasonably strong H-Fe bonding interaction within this  $b_2$  orbital, and this interaction should be maximized when the hydrogen atom is sitting between the iron second-nearest neighbors, i.e., when the hydrogen atoms are in the tetragonal holes of the bcc structure.

While hydrogen adsorption and dissociation may be explained in a fairly straightforward manner by molecular-orbital theory, attempts to explain embrittlement at the molecular level must be assisted by considering embrittlement as a competitive process

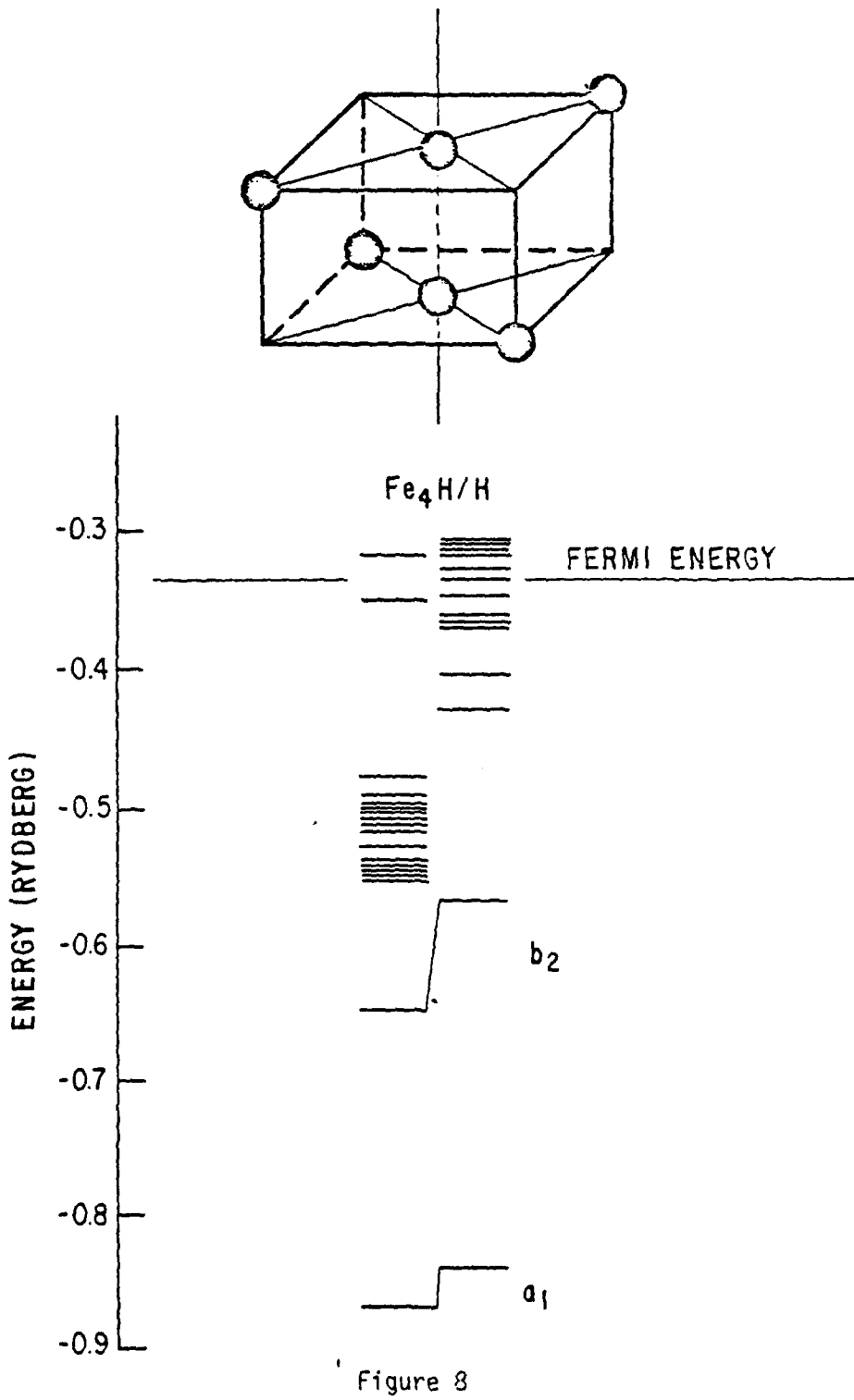


Figure 8

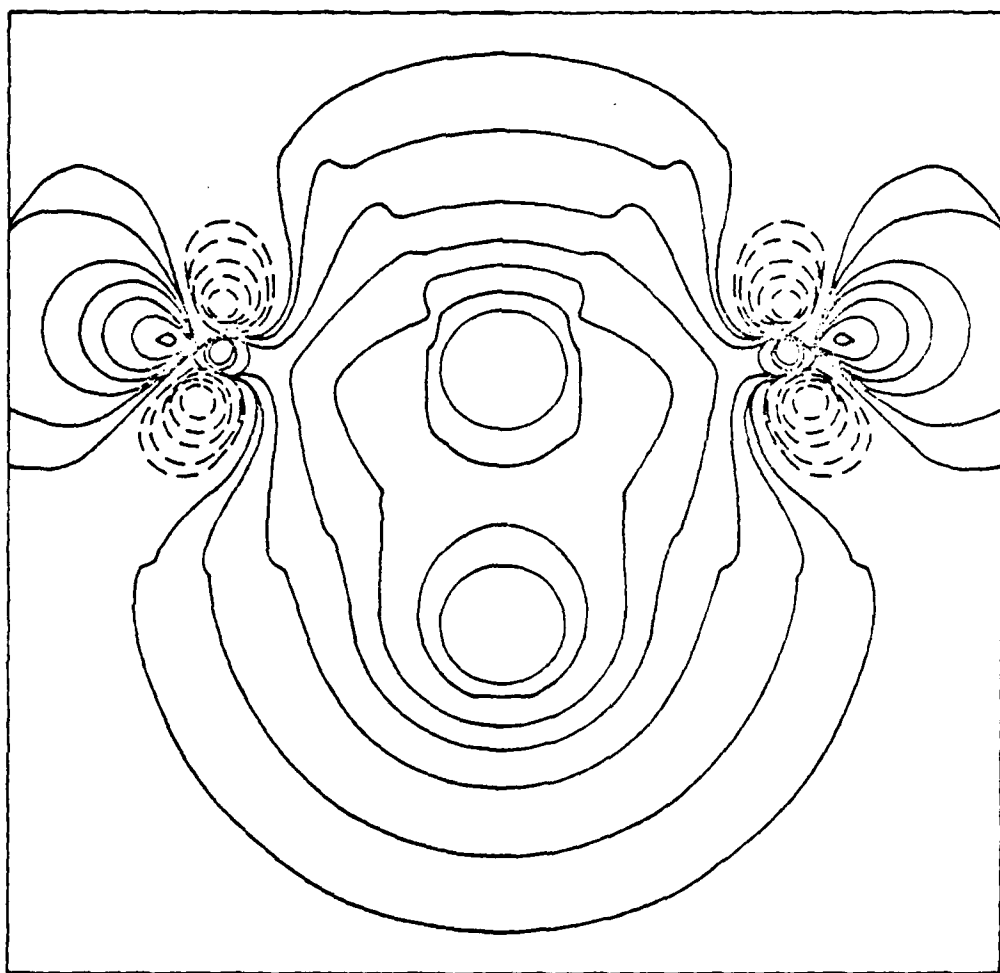


Figure 9

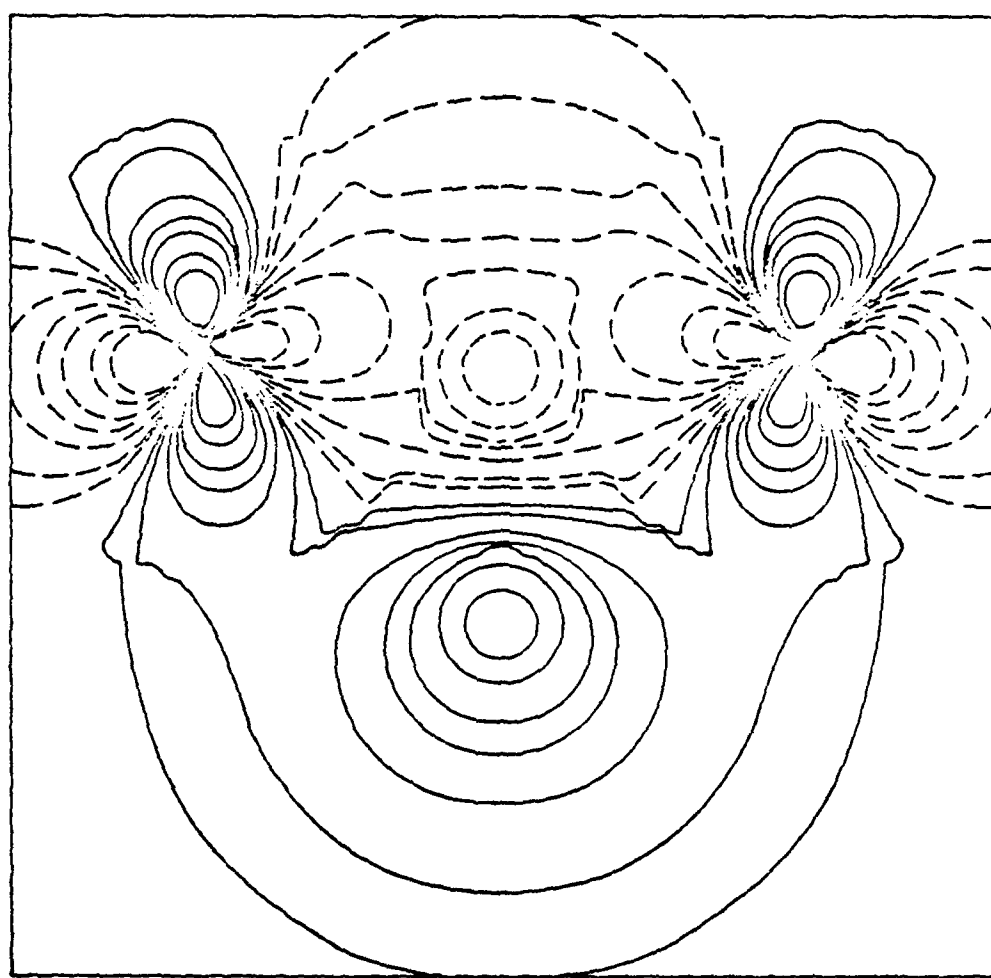


Figure 10

between two mechanisms. The first of these is the process of plastic flow facilitated by dislocation movement. The second is characterized by nuclear motion in a direction which will counter the strain energy of the crystal, a purely elastic response. An energy of activation may be associated with each of these processes. The activation energy for the first process will depend preeminent upon the structure of the crystal, the Burgers vector, etc., while the activation energy of the second process is simply the fracture energy of the crystal. A ductile metal responds to excessive strain through the first mechanism, and this may be attributed to the fact that the activation energy for plastic flow is significantly less than the activation energy for brittle fracture. A brittle material will respond to strain by fracturing before plastic flow begins because the activation energy for dislocation movement is higher than the activation energy for brittle fracture. A ductile-brittle transition must be the result of a mechanism that either raises the activation energy for plastic flow or lowers the energy for brittle fracture.

If the process of hydrogen adsorption affects the activation energy for dislocation flow, then hydrogen adsorption must alter the structure of bcc iron. Structural changes are often manifest as changes in the molecular orbital energy distribution near the Fermi level. Figure 11 shows the molecular orbital energy distribution near the Fermi level for a tetrahedron of iron atoms, the four-atom cluster modeling bcc iron, and three-hydrogenated-iron cluster corresponding to adsorbed molecular hydrogen, adsorbed dissociated molecular hydrogen and a hydrogen saturated cluster,  $\text{Fe}_4\text{H}_6$ . In the tetrahedral cluster, there is an unoccupied  $t_2$  orbital near the Fermi level, this orbital is split when the symmetry of the cluster is reduced from tetrahedral to  $D_{2d}$  as in the 4-atom bcc cluster. The  $e$  orbital is stabilized and becomes occupied while the  $b_2$  orbital is destabilized. This process is reminiscent of the Jahn-Teller effect of inorganic complexes, where a complex spontaneously distorts in order to lower its total energy. This leads to the conjecture that the bcc structure of iron is a consequence of a Jahn-Teller distortion of a fcc structure. When hydrogen molecules are added to the bcc cluster the  $e$  orbital is depopulated and is nearly degenerate with the  $b_2$  orbital, and is similar to the energy distribution of the tetrahedral iron cluster. The dissociation of the hydrogen molecule stabilizes the  $b_2$  orbital but the addition of more hydrogen seems once again to depopulate this orbital. Hydrogen adsorption would appear to promote a close-packed phase transition near the site of adsorption. There is evidence that hydrogen adsorption does promote phase transformations. In HCP iron hydrogen adsorption is known to lower the stacking fault energy indicating that hydrogen is promoting the fcc-hcp phase transition.

This is just the type of effect that would raise the

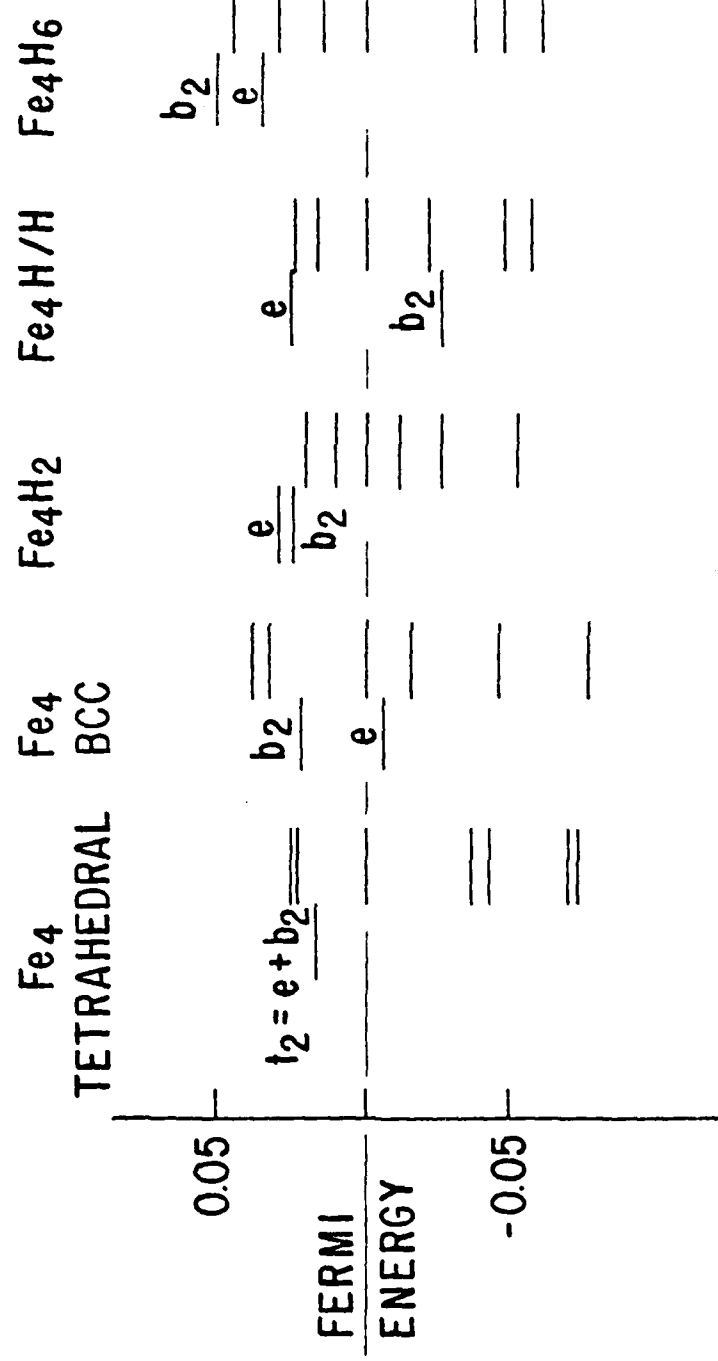


Figure 11

activation energy for dislocation movement around the sites of hydrogen adsorption. However, no surface reconstruction of iron due to hydrogen adsorption has ever been noted and fcc metals, notably nickel, embrittle in a hydrogen environment. While hydrogen undoubtedly has an effect on the structure of bcc iron, it is unlikely that this alone can account for hydrogen embrittlement.

This leaves the possibility that hydrogen adsorption lowers the activation energy of brittle fracture. If this is the case then hydrogen-adsorbed clusters should have molecular orbitals that show similarities to metal clusters that have been strained, for such clusters require less additional energy to fracture, i.e., the activation energy for brittle fracture has been lowered. Accordingly, the molecular orbital energy levels for the four-atom bcc cluster in which the iron atoms have been strained 20% along the twofold rotation axis was calculated. The relative energy distribution of the majority spin states for this cluster is shown in Fig. 12, along with the four-atom model of bcc iron and the dissociated molecular hydrogen-iron clusters. (The minority spin states for all clusters show the same ordering of the energy levels as do the majority spin states. No information is lost by studying only the majority spin states, while the forest of levels is considerably thinned.)

The process of straining the bulk material results in considerable rearrangement of the energy levels within the energy manifold. A rough measure of the difference between two energy manifolds is the number of intersections between the connecting lines of the manifolds. There are ten intersections between the bulk and the strained material, while there are only two intersections connecting the strained and the hydrogenated-iron energy manifolds. Saturation of the  $Fe_4$  cluster with hydrogen results in almost no rearrangement of the energy manifold. What rearrangement occurs is confined to the lowest five orbitals of the manifold.

The direction in which the molecular-orbital energy levels move upon straining can be seen to be the result of removing electron density from between nearest neighbors, and replacing it in the region perpendicular to the direction of strain, i.e., between second-nearest neighbors. The result should be a contraction of the cluster perpendicular to the direction of strain. This is the Poisson effect. Within this analysis it is clear that hydrogen atoms in tetragonal holes will mimic the behavior of strain by increasing the electron density between second-nearest neighbors. It is worth noting that only the two lowest lying orbitals of the hydrogenated-iron cluster have any hydrogen admixture; therefore, the rearrangement of the other orbitals must be the result of a relaxation effect due to the stabilization of the lowest  $a_1$  and  $b_2$  orbitals.

It seems reasonable then that if the lowest lying  $a_1$  and  $b_2$

$\text{Fe}_4$        $\text{Fe}_4$        $\text{Fe}_4\text{H}/\text{H}$   
20% STRAINED

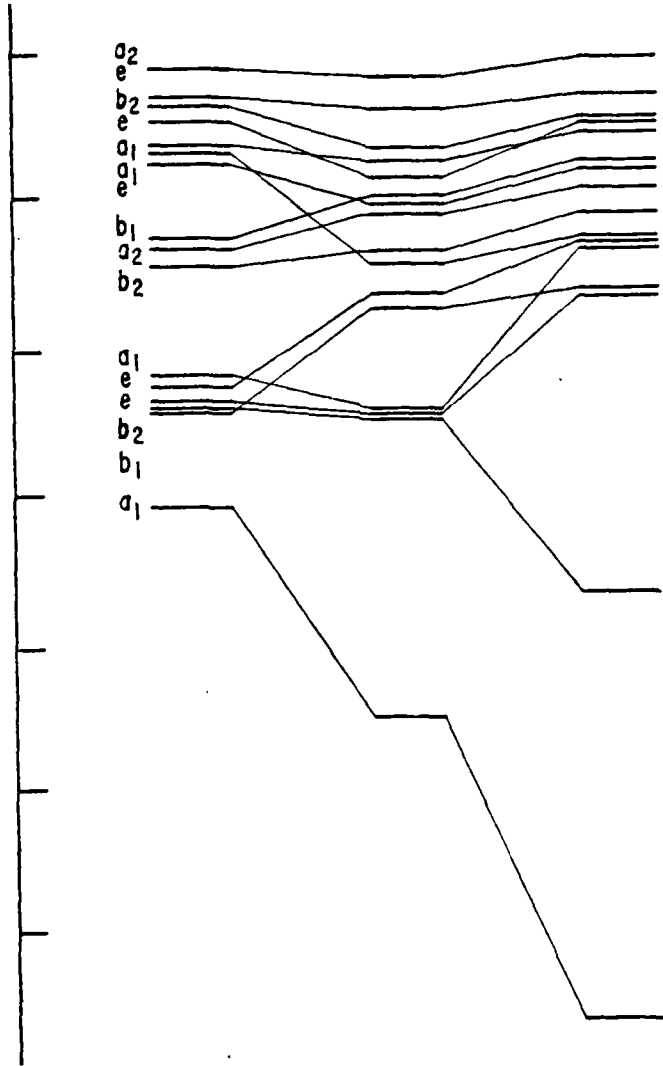


Figure 12

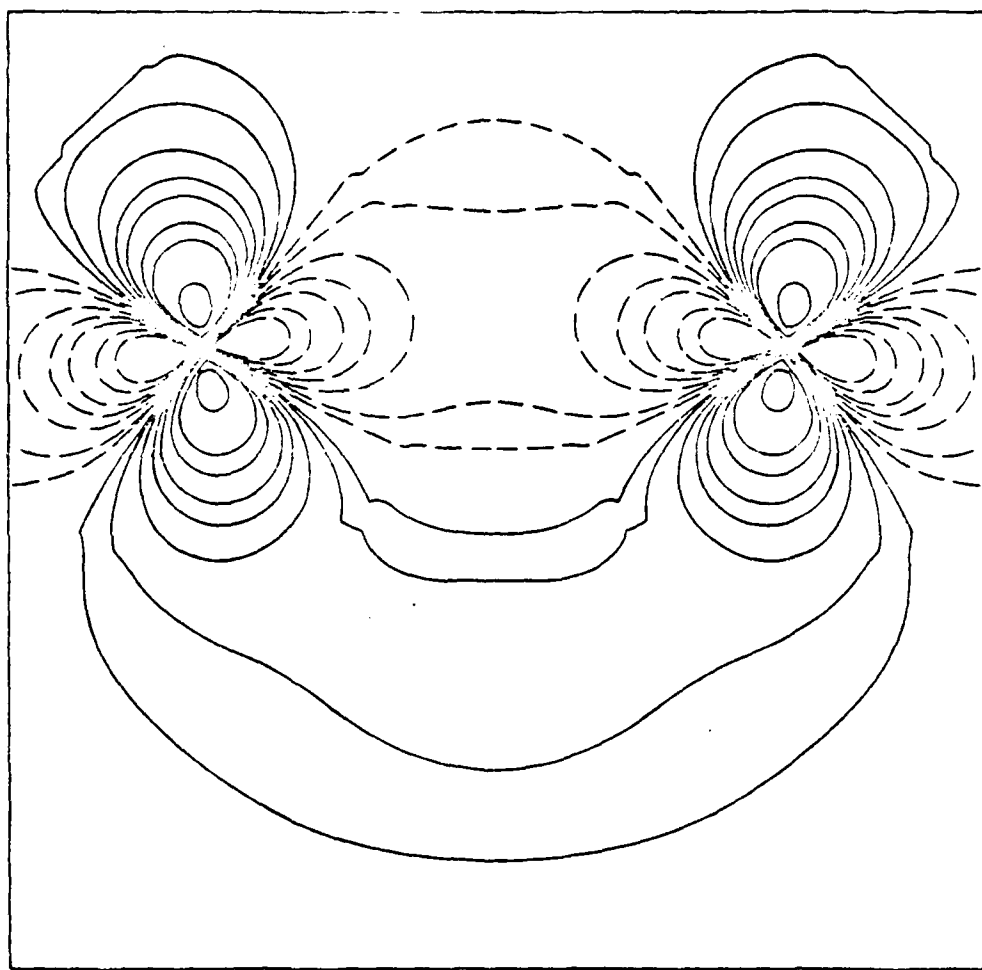


Figure 13

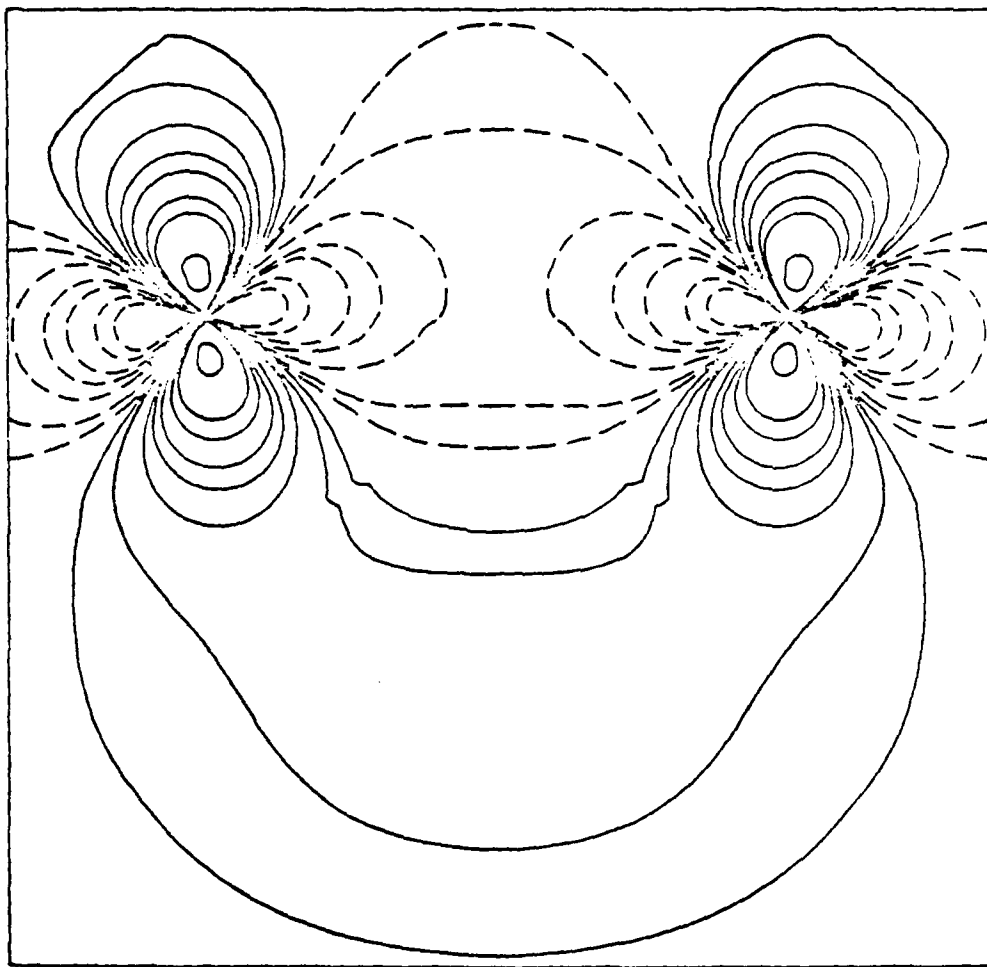


Figure 14

orbitals of the strained and hydrogenated cluster are similar in composition, the other orbitals of the manifold should also show similarities. Figures 13 and 14 compare the lowest  $b_1$  orbitals in an xz plane containing the second neighbors for the unstrained and strained (20%) Fe<sub>9</sub> clusters, respectively. Again, both the hydrogen-adsorbed (Fig. 10) and strained cluster (Fig. 14) show greater electron density between second neighbors and even similar electron distributions in areas away from the hydrogen atom.

#### ACKNOWLEDGMENTS

This work was supported in its entirety at M.I.T. and in part at G.E. by research grants provided by the Office of Naval Research.

